Supporting Information for

Concurrent alloying and vacancy engineering for intensifying

hydrogen spillover towards alcohol–water co-electrolysis

Hui Xu, Kun Wang, Guangyu He[*], Haiqun Chen[*]

Key Laboratory of Advanced Catalytic Materials and Technology, Advanced

Catalysis and Green Manufacturing Collaborative Innovation Center, Changzhou

University, Changzhou, Jiangsu Province 213164, China

Corresponding authors: hegy@cczu.edu.cn (G. He); chenhq@cczu.edu.cn (H. Chen)

Computational method

All the DFT calculations are performed by the Vienna Ab initio Simulation Package (VASP) [1] with the projector augmented wave (PAW) method [2]. The exchange-functional is treated using the generalized gradient approximation (GGA) of Perdew-Burke-Ernzerhof (PBE) [3] functional. The energy cutoff for the plane wave basis expansion was set to 400 eV and the force on each atom less than 0.05 eV/Å was set for convergence criterion of geometry relaxation. Partial occupancies of the Kohn−Sham orbitals were allowed using the Gaussian smearing method and a width of 0.2 eV. The interface between RuO_2 and Ru/PdRu was built, named as $Ru-RuO_2$ and $PdRu-RuO_2$, respectively. The Brillouin zone was sampled with Monkhorst mesh of $1\times1\times1$. The self-consistent calculations apply a convergence energy threshold of 10^{-4} eV and a force convergency of 0.05 eV/Å. The H-transfer process was simulated using the climbing image nudged elastic band (ci-NEB) method [4]. The reaction free energy for elementary steps in HER were calculated based on the computational hydrogen electrode (CHE) approximation [5].

The free energy corrections were considered at the temperature of 298 K, following:

$$\Delta G = \Delta E + \Delta G_{ZPE} + \Delta G_U - T\Delta S$$

where ΔE, ΔG_{ZPE}, ΔG_U, and ΔS refer to the DFT calculated energy change, the correction from zero-point energy, the correction from inner energy and the correction from entropy [6].
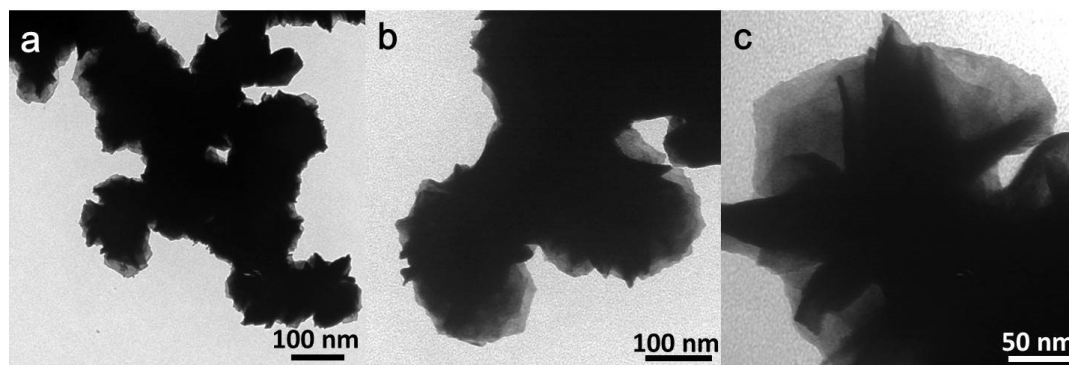
Fig.S1 TEM images of the metallene-like Pd nanostructures with different
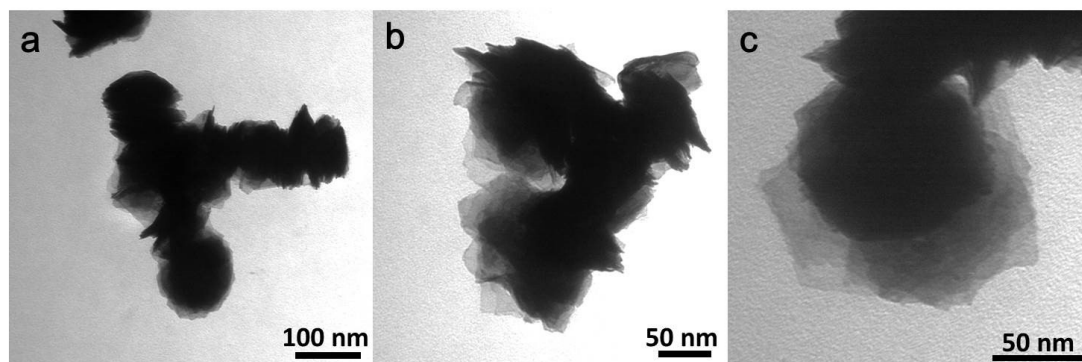
magnifications.

Fig.S2 TEM images of the metallene-like PdCu nanostructures with different magnifications.

Fig.S3 STEM image of the metallene-like PdRu-RuO$_2$ nanostructure.
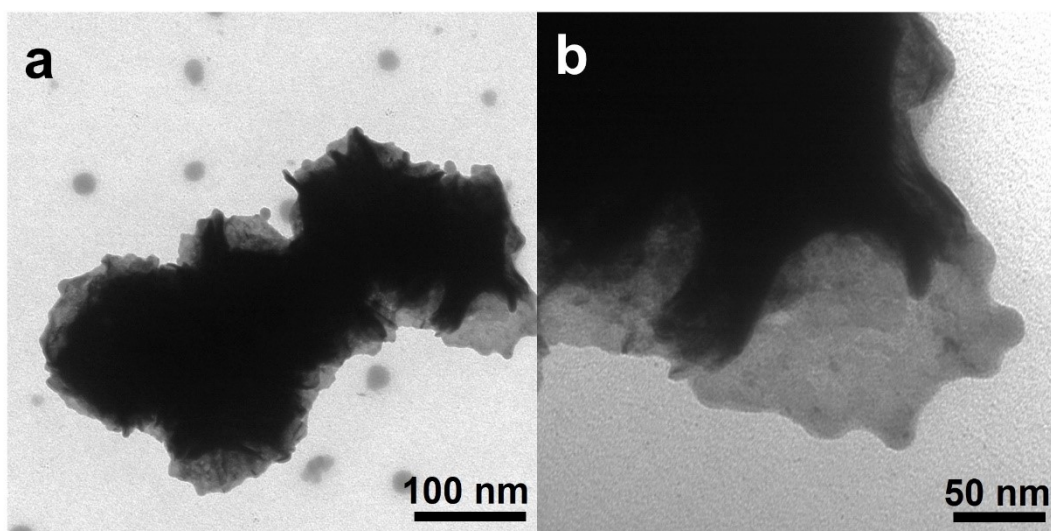
Fig.S4 TEM image of the metallene-like PdRu-RuO$_2$ nanostructure with different magnifications.
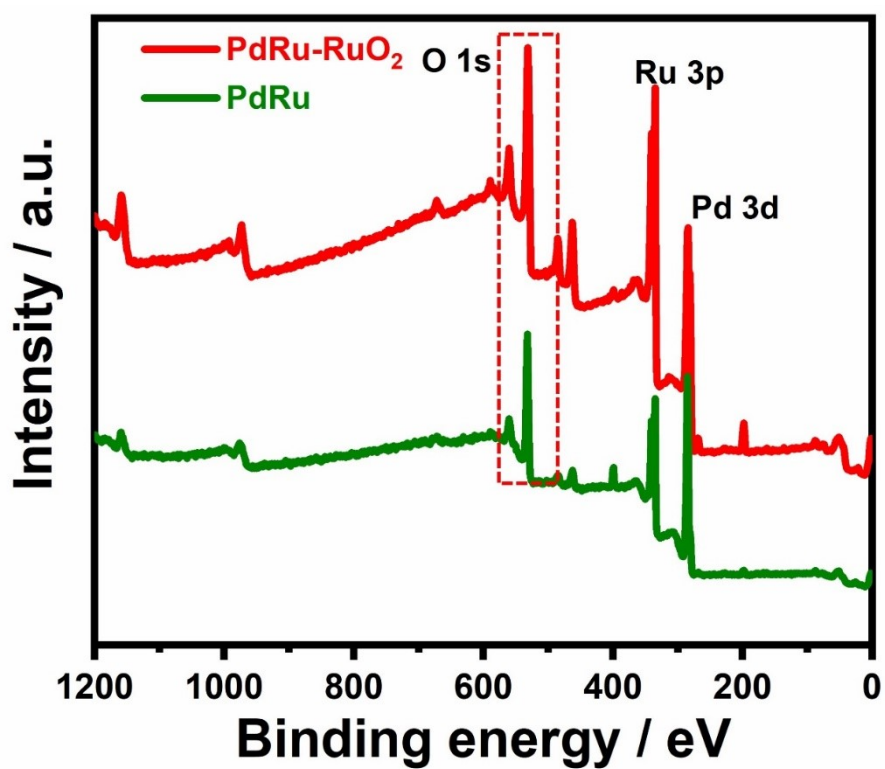
Fig.S5 XPS survey spectra of the PdRu-RuO$_2$ and PdRu nanostructure.
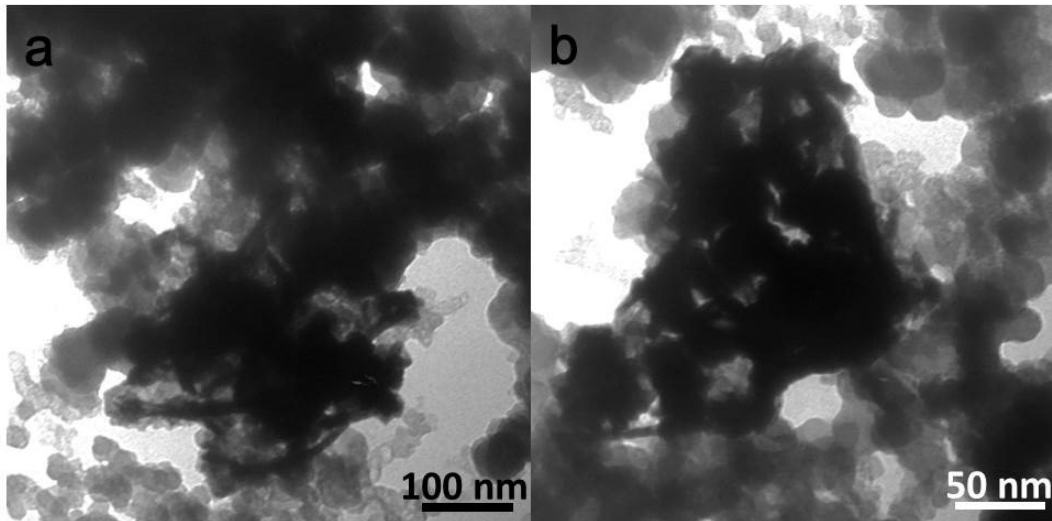
Fig.S6 TEM image of the carbon black loaded PdRu-RuO$_2$ nanostructure.
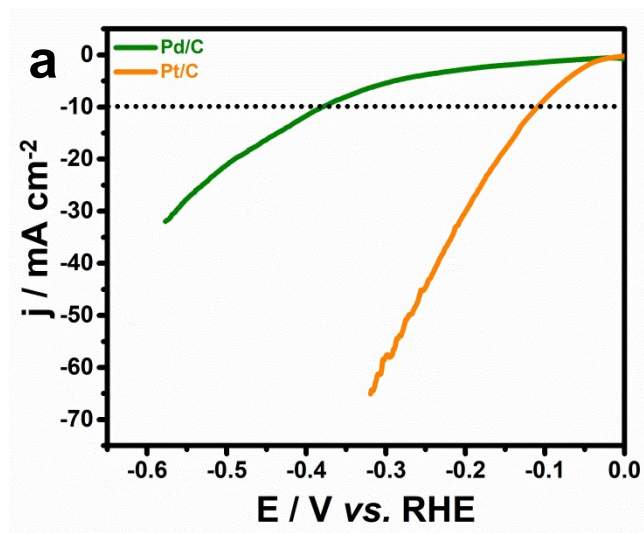
Fig.S7 LSV polarization curves of Pd/C and Pt/C in 1 M KOH solution.
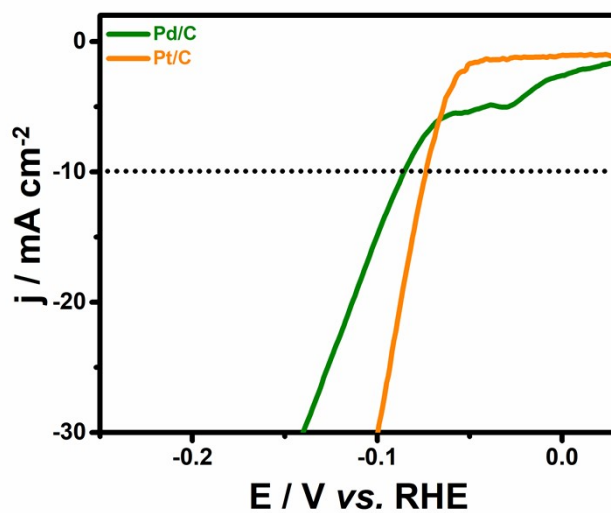
Fig.S8 LSV polarization curves of Pd/C and Pt/C in 0.5 M H$_2$SO$_4$ solution.
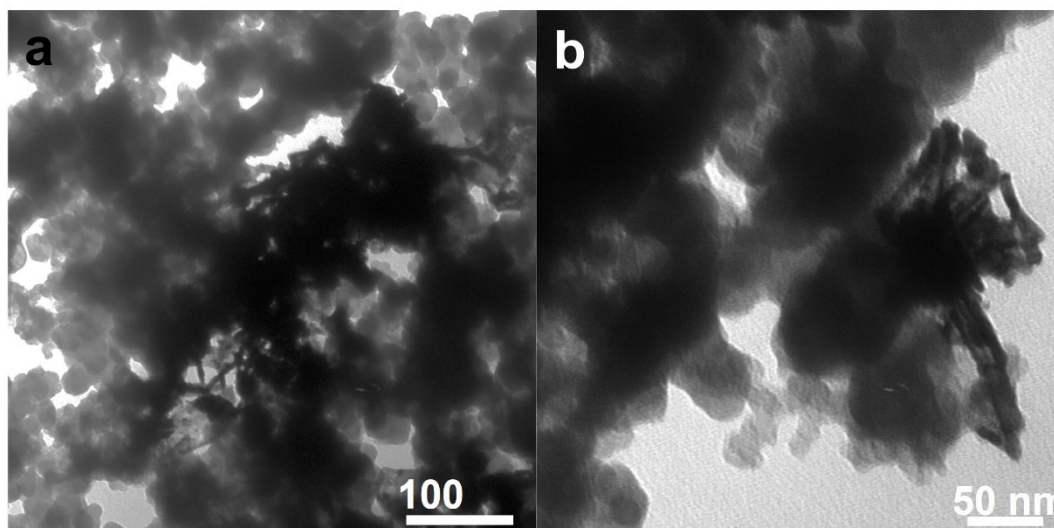
Fig.S9 TEM image of the carbon black loaded PdRu-RuO$_2$/C after long-time electrochemical operation.
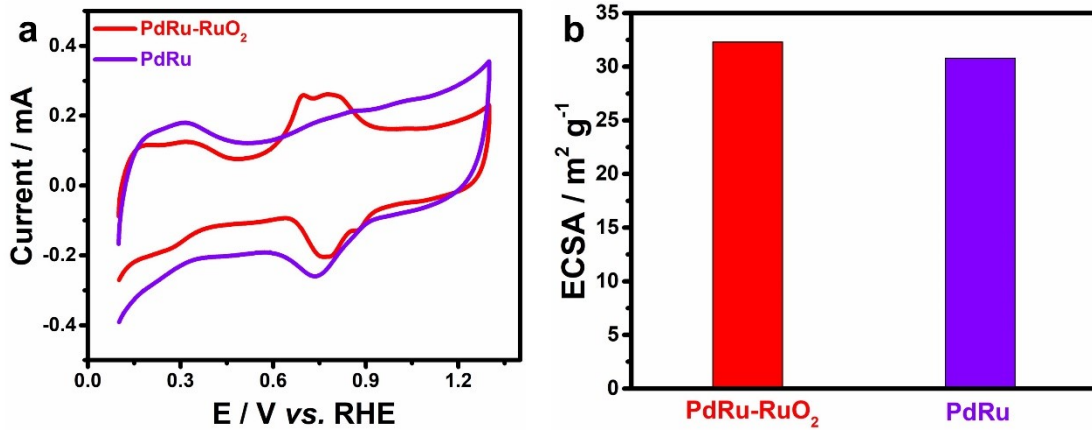
Fig.S10 (a) CV curves of PdRu-RuO$_2$/C and PdRu/C in 1 M KOH solution. **(b)** Histograms for the ECSA of PdRu-RuO$_2$/C and PdRu/C.
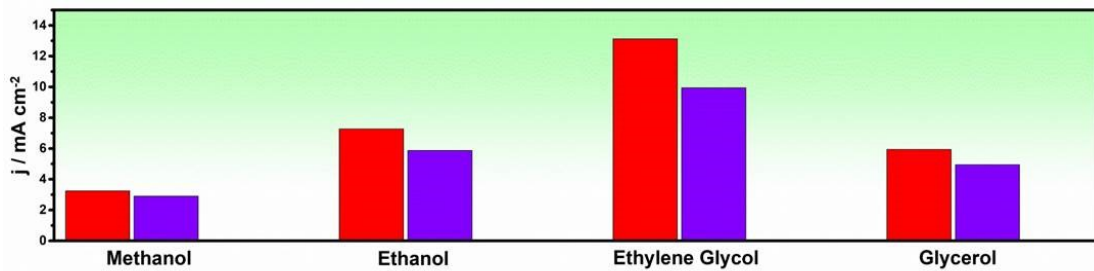
Fig.S11 Histogram for the specific activities of MOR, EOR, EGOR, and GOR catalyzed by PdRu-RuO$_2$/C and PdRu/C.
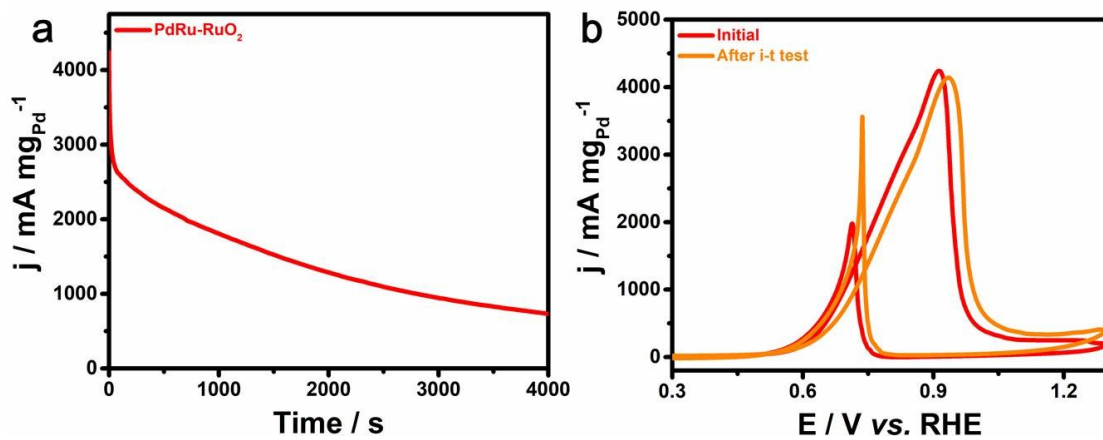
Fig.S12 (a) i-t curve of PdRu-RuO$_2$/C for EGOR. (b) CV curves of PdRu-RuO$_2$/C before and after i-t test.
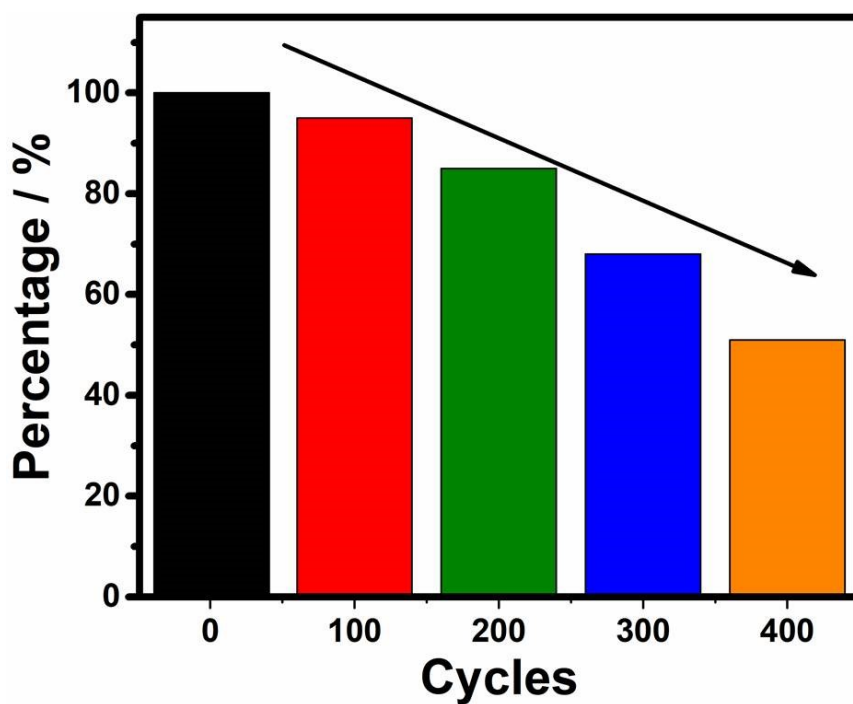
Fig.S13 Histogram of the percentage of mass activity when normalized with the oxidation peak current.
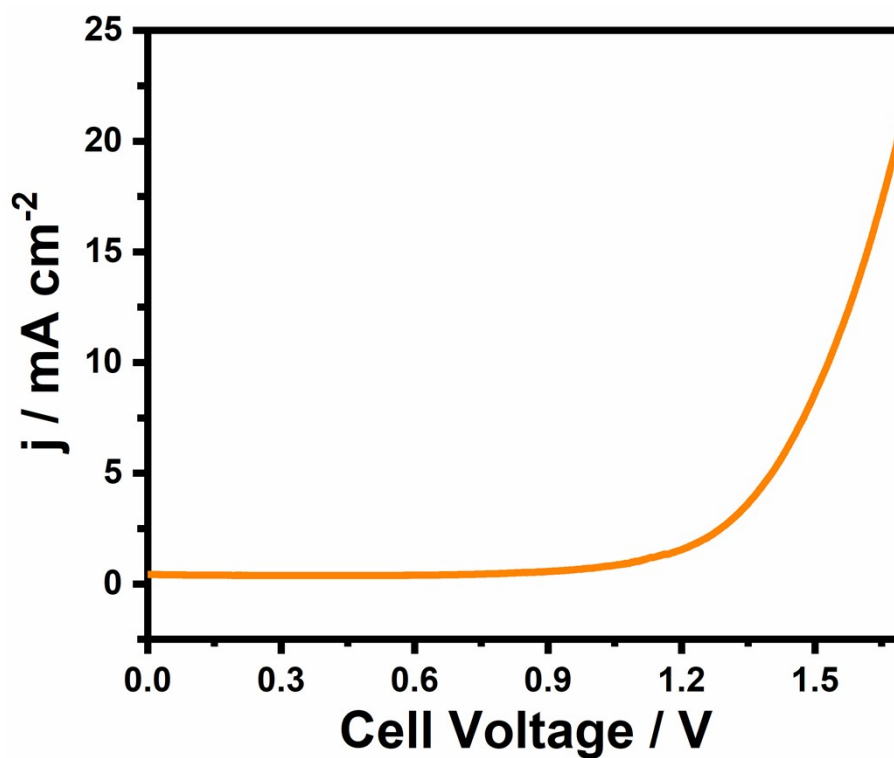
Fig.S14 LSV curve of PdRu-RuO$_2$/C for driving overall water splitting in 1 M KOH

electrolyte.
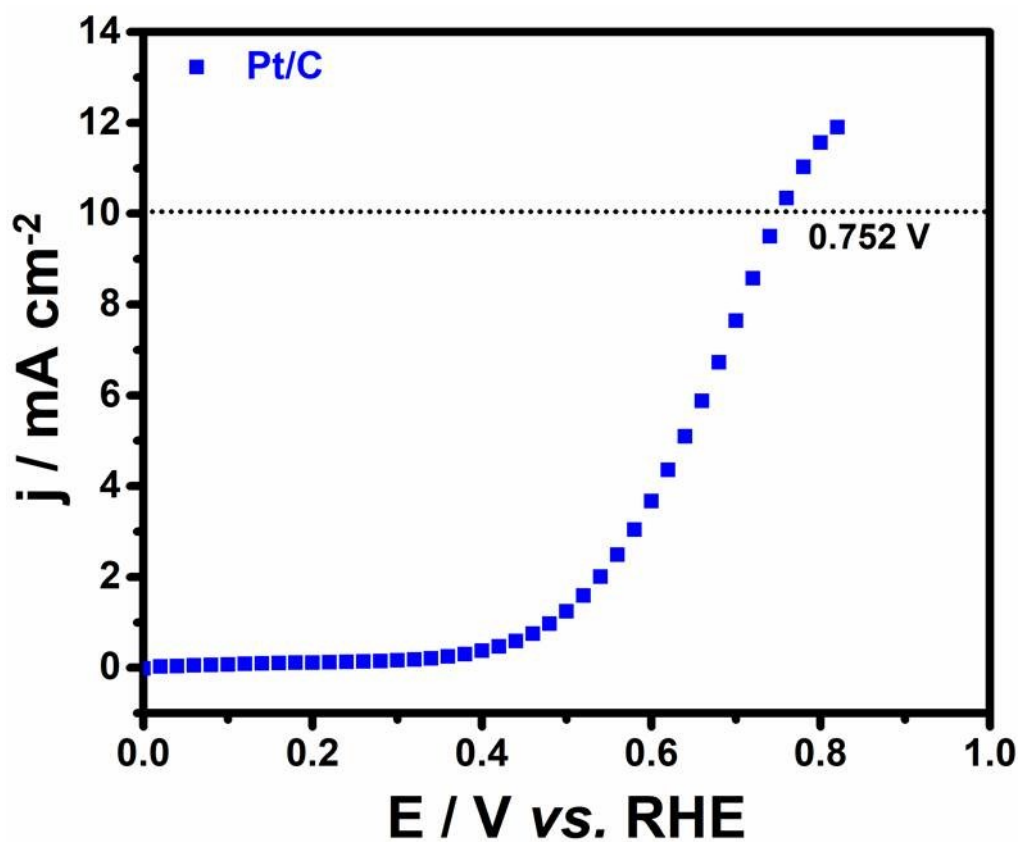
Fig.S15 LSV curve of Pt/C for driving HER and EOR in an aqueous solution containing 1 M KOH and 1 M CH₃CH₂OH.
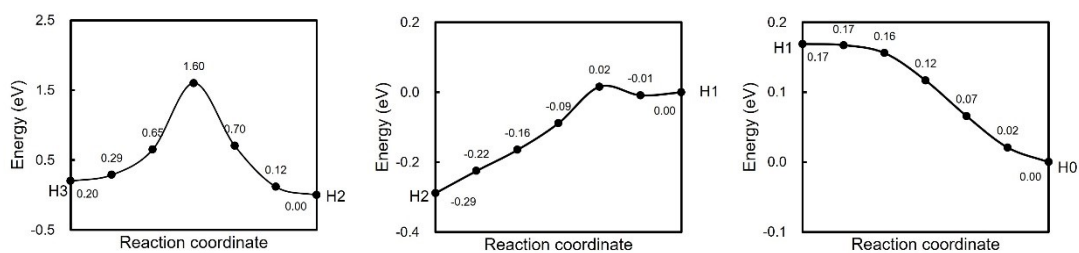
Fig.S16 Hydrogen transfer energy of different active sites based on PdRu-RuO₂.
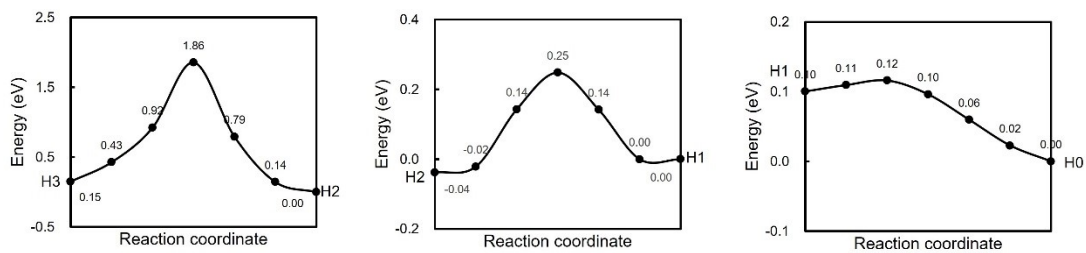
Fig.S17 Hydrogen transfer energy of different active sites based on Ru-RuO$_2$.
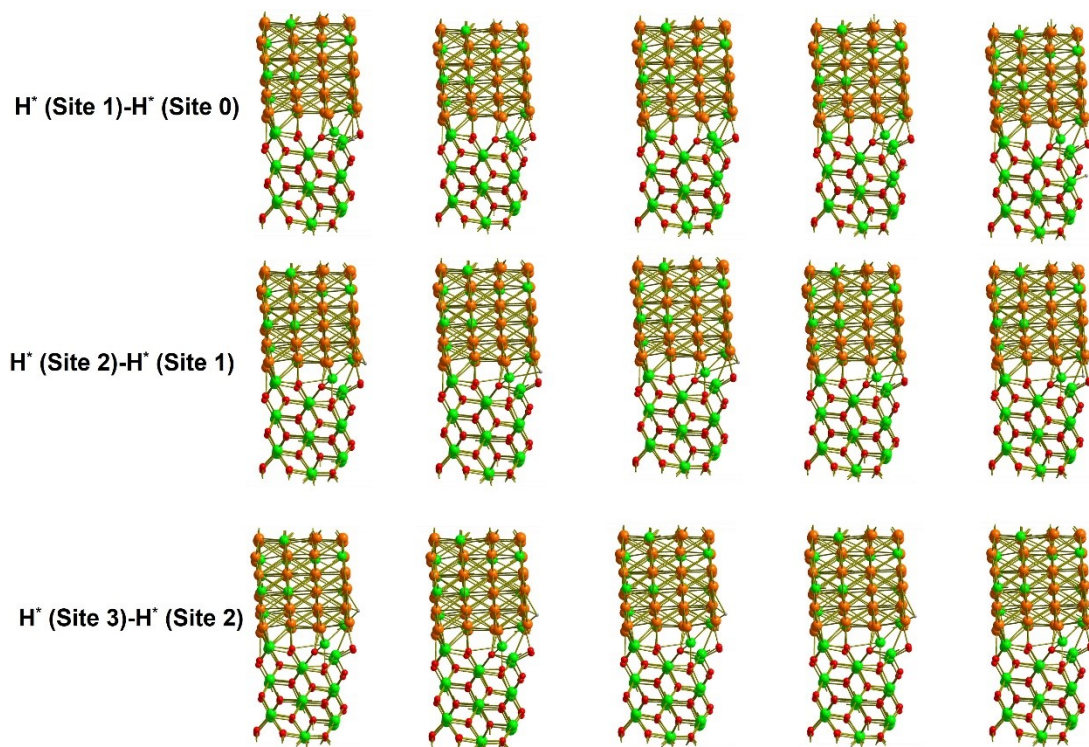
Fig.S18 Hydrogen spillover process of different active sites based on PdRu-RuO$_2$.
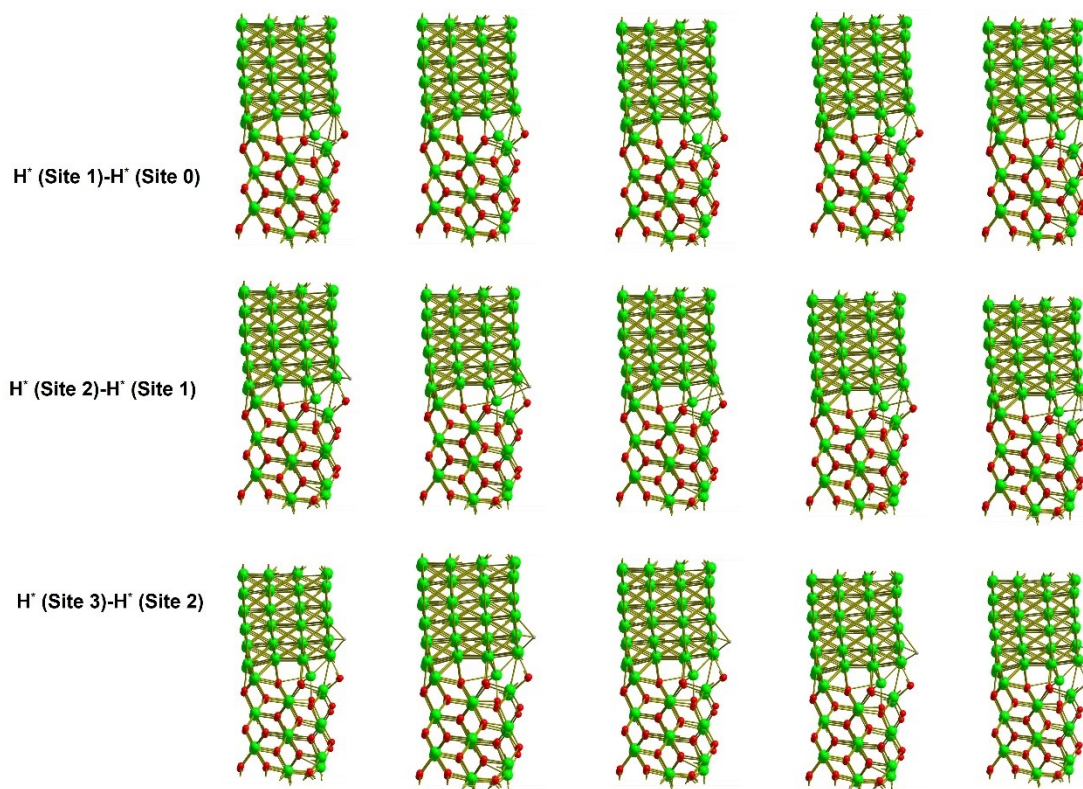
Fig.S19 Hydrogen spillover process of different active sites based on Ru-RuO$_2$.

Table S1 Summary of the work functions of different materials

Catalyst	Work function (eV)
Pd	5.12
Ru	4.71
PdRu	5.05
RuO$_2$	5.13

References

[1] Kresse, G.; Furthmüller, J. Comp Mater Sci 1996, 6, (1), 15-50.

[2] Blöchl, P. E. Phys. Rev. B 1994, 50, (24), 17953-17979.

[3] Perdew, J. P.; Chevary, J. A.; Vosko, S. H.; Jackson, K. A.; Pederson, M. R.; Singh, D. J.; Fiolhais, C. Phys. Rev. B 1992, 46, (11), 6671-6687.

[4] Henkelman, G.; Uberuaga, B. P.; Jónsson, H., A climbing image nudged elastic band method for finding saddle points and minimum energy paths. The Journal of Chemical Physics 2000, 113 (22), 9901-9904.

[5] Nørskov, J. K.; Rossmeisl, J.; Logadottir, A.; Lindqvist, L.; Kitchin, J. R.; Bligaard, T.; Jónsson, H., Origin of the Overpotential for Oxygen Reduction at a Fuel-Cell Cathode. The Journal of Physical Chemistry B 2004, 108 (46), 17886-17892.

[6] Guo, C.; Tian, X.; Fu, X.; Qin, G.; Long, J.; Li, H.; Jing, H.; Zhou, Y.; Xiao, J., Computational Design of Spinel Oxides through Coverage-Dependent Screening on the Reaction Phase Diagram. ACS Catalysis 2022, 12 (11), 6781-6793.